Mechanical Systems and Signal Processing 213 (2024) 111339



Contents lists available at ScienceDirect

Mechanical Systems and Signal Processing

journal homepage: www.elsevier.com/locate/ymssp





Coded excitation using TOP-CS sequences for multi-channel low-power ultrasonics

Connor Challinor [a], Neil Pearson [b], Frederic Cegla [a,*]

[a] Department of Mechanical Engineering, Imperial College London, Exhibition Road, South Kensington, London, SW7 2AZ, UK
[b] Eddyfi Technologies, Clos Llyn Cwm, Swansea, SA6 8QY, UK

ARTICLE INFO

Communicated by M. Rebillat

Keywords:
Coded excitation
Phase modulation
Sequence orthogonality
Ultrasonics

ABSTRACT

This paper presents a low-power hardware architecture that facilitates the simultaneous transmission and reception of ultrasonic signals when using coded excitations for ultrasonic measurements. With this architecture, long pseudo-periodic coded excitations, which have previously been unsuitable for pulse-echo measurements, can be used to produce high Signal-to-Noise Ratio (SNR) results without an increase in signal dead-zone and without introducing filter artefacts within a set measurement window. We show that a low-power system (±2 V peak excitation amplitude without receiver amplification) utilising such coded excitations can achieve the same level of performance as a conventional high-power system (−200 V peak excitation amplitude with 15 dB receiver amplification) by producing 45 dB SNR measurements whilst maintaining a high Pulse Repetition Frequency (PRF) of ≥0.5 kHz. The use of pseudo-periodic sequences to produce quasi-orthogonal sequence families is then demonstrated to allow an arbitrary number of acquisition channels to be used simultaneously with complete crosstalk removal within a set measurement window. Therefore, the work presented here can open the door for the development of simplified low-power multi-channel acquisition systems without sacrificing system performance.

1. Introduction

Pulse compression techniques have been researched extensively for improving signal quality across several active ranging applications [1], such as radar [2–5], ultrasonic non-destructive evaluation (NDE) [6–23], and ultrasonic medical imaging [24–42]. Pulse compression techniques involve employing modulated excitation signals to increase energy delivery through extended transmission durations. In ultrasonic measurements, the Signal-to-Noise Ratio (SNR) is proportional to the total excitation energy [43,44], assuming noise is present as Additive White Gaussian Noise (AWGN). Therefore, by maximising energy delivery, high-quality signals can be acquired. However, short excitation pulses are often preferred as they maximise temporal resolution, thus leaving traditional excitation techniques to rely on narrow high amplitude excitations to achieve sufficient energy delivery. Pulse compression techniques were first developed to help avoid the need for high voltage pulsers, which are typically one of the least efficient components in an acquisition system [45]. By utilising modulated signals that exhibit time compression when convolved against their time inverse, pulse compression techniques can effectively utilise increased transmission durations without sacrificing temporal resolution.

The most common modulations used for pulse compression are variations of a signal's frequency or phase throughout the signal duration. Coded excitations are a subset of pulse compression based excitations that focus on the use of phase modulations. A coded

* Corresponding author.
E-mail address: f.cegla@imperial.ac.uk (F. Cegla).

https://doi.org/10.1016/j.ymssp.2024.111339
Received 12 October 2023; Received in revised form 24 January 2024; Accepted 11 March 2024
Available online 16 March 2024
0888-3270/© 2024 The Author(s). Published by Elsevier Ltd. This is an open access article under the CC BY license (http://creativecommons.org/licenses/by/4.0/).

excitation signal uses a fixed excitation pulse, referred to here as a symbol, which is transmitted consecutively with a varying start phase. The start phase is most commonly set through binary sequences (sequences comprising 1's and 0's or 1's and −1's), often termed the 'code', of which several options are available [1,46]. Through sequence design optimisation, coded excitation can yield substantial improvements in SNR without requiring complex acquisition hardware as, in its simplest form, the technique relies only on the generation of bipolar pulses. Further, coded excitation has also been investigated for use in suppressing crosstalk in multi-channel applications, such as ultrasonic phased arrays, by using orthogonal sequence families [33,35–39]. By designing sequence families that exhibit orthogonality (sequences that cancel completely when convolved with the time inverse of each other sequence in the family), families of modulations can be produced such that each transducer in a multi-channel application is assigned its own unique excitation signal that allows it to operate without concern of crosstalk from neighbouring channels.

The typical focus of prior research into using coded excitation for ultrasound acquisitions has been in evaluating how the technique can be used to improve the output from a traditional acquisition system. The increase in SNR achieved from using coded excitation has been shown to allow NDE measurements with reduced transmission amplitudes [14] and in challenging inspection environments where the expected signal quality is lower [7,10,12]. Whilst there are demonstrable benefits of using coded excitation on the traditional system, the need for the traditional system to perform well with standard excitation signals imposes limitations on how well it can adopt phase modulated transmissions. To ensure a high baseline SNR, the traditional system commonly uses a high-voltage transmission architecture combined with an isolated low-voltage reception architecture. Systems utilising this hardware approach are unable to simultaneously transmit and receive energy through a single transducer element given the transmission signals saturate the receiver components. As a result, only short aperiodic sequence based coded excitations are suitable for pulse-echo applications which can greatly reduce the usefulness of the technique. When limited to short aperiodic sequences, SNR gain can be minimal and ideal compression and large family orthogonality cannot be achieved meaning problematic artefacts are introduced to filtered signals. The use of pitch-catch configurations with separate transmission and reception elements can reduce the limitation on applicable sequence lengths and types, but this work is focusing on single- and multi-channel pulse-echo configurations which are more common across ultrasonic NDE and medical applications.

In this paper, the authors are proposing a change in philosophy of how coded excitation is applied. Instead of investigating how coded excitation can be used to improve an existing acquisition system, this work investigates how an alternative acquisition system can uncover untapped potential in how sequence design can be optimised for ultrasound coded excitations. By creating a new acquisition system that facilitates the simultaneous transmission and reception of ultrasonic signals through a single transducer element, the limitation on applicable sequence length is greatly relaxed. With this new system, the sequence length can be increased at will, assuming the system remains stationary, to increase SNR gain with limitations only imposed by the application's required Pulse Repetition Frequency (PRF). Further, pseudo-periodic sequences can be introduced such that single-shot acquisitions can produce artefact free compression within a set measurement window. An extension of pseudo-periodic sequences into quasi-orthogonal sequence families can then be utilised to facilitate complete crosstalk removal within a set measurement window for an arbitrary number of measurement channels. This is beneficial in allowing for fully parallel acquisition across elements in multi-channel applications (i.e., phased arrays). With this proposed change in hardware architecture, the use of sequences can be optimised whilst hardware complexity is minimised.

The paper is organised as follows. The limitations of traditional coded excitation with a standard hardware architecture is covered in Section 2. Section 3 introduces an alternative low-power hardware architecture to overcome these limitations and compares this approach combined with traditional sequences to an industry standard high-voltage acquisition system. Section 4 describes a novel type of sequence that utilises pseudo-periodicity to achieve ideal-like compression. Section 5 introduces the circularly-shifted sequence family production method for achieving quasi-orthogonality on an arbitrary number of channels. Section 6 presents experimental results to evaluate the capability of the presented methodology for single- and multi-channel applications. Finally, conclusions on the potential of the proposed low-power coded excitation approach are drawn in Section 7.

2. Traditional coded excitation

In the context of ultrasound measurements, coded excitations are used to increase the total transmitted energy by using temporally long excitation signals which contain phase modulations controlled by typically binary sequences. The sequences are used to dictate the start phase of a symbol such that the total coded excitation signal consists of consecutive symbols with varying start phases. Here, a symbol can range from a single-valued spike/impulse up to complex multi-cycle excitation waveforms. As the modulated component of a coded excitation signal is the symbol's phase, the symbol itself can be any shape depending on the need to simplify hardware or match the transducer bandwidth for improved transmission/reception efficiency. The ability for the symbol to be designed independently to the coded signal's modulation can make the use of phase modulation preferable over alternative pulse compression based excitation signals. Fig. 1 demonstrates the production of a Barker sequence coded excitation through the convolution of a single-cycle bipolar symbol with an up-sampled adaptation of the sequence itself (up-sampling is used to ensure symbol overlap is avoided during the convolution).

When using a coded excitation signal that contains an ideal modulation, $\psi(t)$, complete time-domain compression can be achieved without introducing filter artefacts by convolving, $\otimes$, signals against the time inverse of the coded excitation itself, $\psi(-t)$ (matched filtering). This is shown in Eq. (1) in which an impulse (denoted as a dirac delta, δ) is recovered following matched filtering of the ideal modulation. Through the compression of energy in the time domain, the impulse recovered has an increased intensity proportional to the energy contained within the modulated signal, denoted as a gain G. Applying such a coded excitation that produces ideal compression to an ultrasound inspection allows for the temporally long excitation to produce a high SNR signal

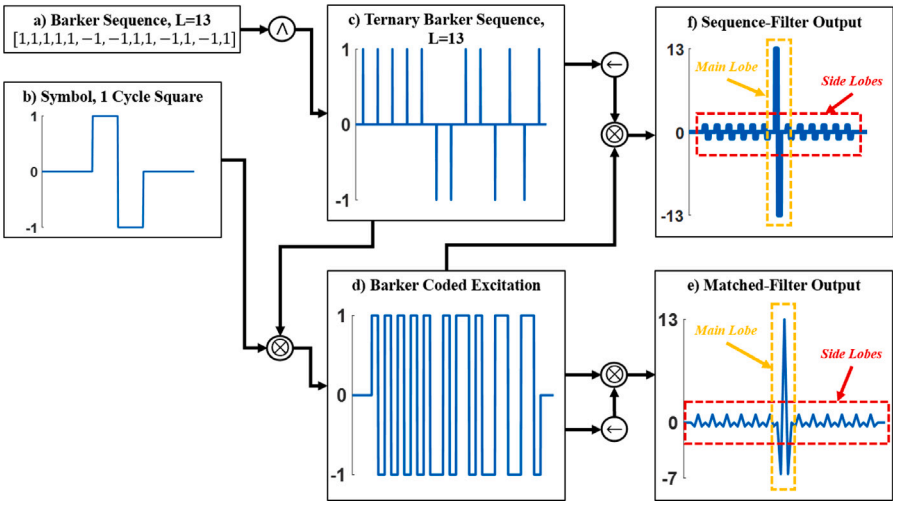


Fig. 1. Showing the creation of Barker Sequence Coded Excitations *(d)* by convolution of a square wave symbol *(b)* and the ternary representation of a Barker Sequence *(c)*. The Coded Excitation's matched-filter response *(e)* is shown to demonstrate the production of a Main Lobe and Side Lobes. The sequence-filter response *(f)* is shown to highlight the difference between the two filter options. ⊗ represents the convolution operator, ← represents reversal in the time domain, and ∧ represents up-sampling and ternary conversion.

without having sacrificed range resolution. The SNR from such a coded excitation based measurement will be L times greater than if coded excitation is not used (but matched filtering is used), where L is the length of the sequence used to create the ideal modulation and therefore defines the increase in transmission energy that results from using the coded excitation.

$$\psi(t) \otimes \psi(-t) = G \times \delta \tag{1}$$

A further use of coded excitation is the ability to suppress crosstalk in multi-channel applications (referred to here as MIMO applications, multiple-in–multiple-out), such as phased array measurements. Creating coded excitations that contain unique modulations for each channel which are all based on ideal orthogonal sequence families allows for multiple measurement channels to operate independently without concern of crosstalk. Orthogonality here is the principle that each sequence within the family cancels completely when cross-filtered against each other — see Eq. (2) in which orthogonality is demonstrated using two ideal modulations, $\psi_1(t)$ and $\psi_2(t)$. With an ideal sequence family, each measurement channel can recover information relating only to its own excitation signal following matched-filtering as all other information will be cancelled. Similarly, the information passing between measurement channels can itself be isolated following appropriate cross-filtering. When using ideal orthogonal coded excitation families, MIMO applications do not require time-consuming staged excitations across channels, as is required with traditional excitation techniques, as post-acquisition signal processing can remove cross-channel distortions arising from ultrasonic crosstalk.

$$\begin{aligned}
\psi_1(t) \otimes \psi_1(-t) &= G \times \delta \\
\psi_1(t) \otimes \psi_2(-t) &= 0 \\
\psi_2(t) \otimes \psi_1(-t) &= 0 \\
\psi_2(t) \otimes \psi_2(-t) &= G \times \delta
\end{aligned} \tag{2}$$

In practice, coded excitations with band-limited symbols that produce ideal compression and orthogonality do not exist. Instead, coded excitations produce time-domain compression in the form of a Main Lobe (ML) which is surrounded by filter artefacts called Side Lobes (SLs). Similarly, Cross Lobes (CLs) are introduced when sequence orthogonality is not met. The shape, amplitude, and position of all lobes is determined by the symbol used, the sequence used and the type of filter used. Two filter options exist, either fully matched which maximises SNR or sequence only that removes the symbol bandwidth filtering, the difference between the filter types is shown in Fig. 1. The Barker sequence used to produce the coded excitation in Fig. 1 produces the greatest Merit Factor of a sequence this length [47] — Merit Factor being the ratio between energy in the ML to energy in all SLs and is a useful metric in evaluating the suitability of a sequence for use in producing coded excitations [48]. Despite a high Merit Factor, the presence of SLs is easily noted in the filter output as shown in the figure. Performing acquisitions with this coded excitation will result in all recorded echoes being surrounded by SL distortions which will greatly complicate further signal analysis. Fig. 2 shows a family of two pseudo-noise sequences and their respective matched-filter and cross-filter outputs as to highlight the presence of CLs when sequence orthogonality is not achieved.

When using coded excitation in active ranging applications, the goal is to find the optimal sequence for maximising energy delivery (longest possible sequence to enable the greatest gain in SNR) and minimising lobe distortions. Sequence design for optimal compression and orthogonality is an ongoing research topic with many parameters determining what can be considered optimal [1].

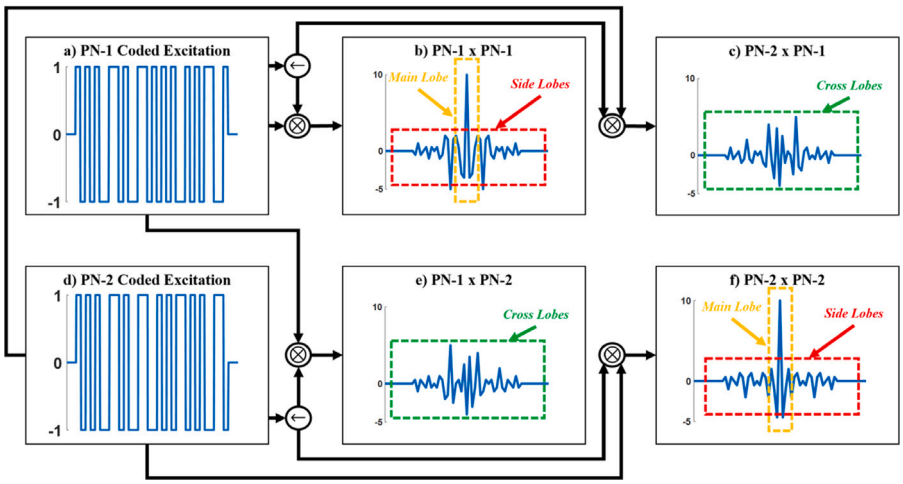


Fig. 2. The use of families of coded excitations, *(a)* and *(d)*, in producing time-domain compression when matched-filtered, *(b)* and *(f)*, and in producing time-domain suppression when cross-filtered, *(c)* and *(e)*. Pseudo-noise sequences of length $L = 10$ used to produce the coded excitations.

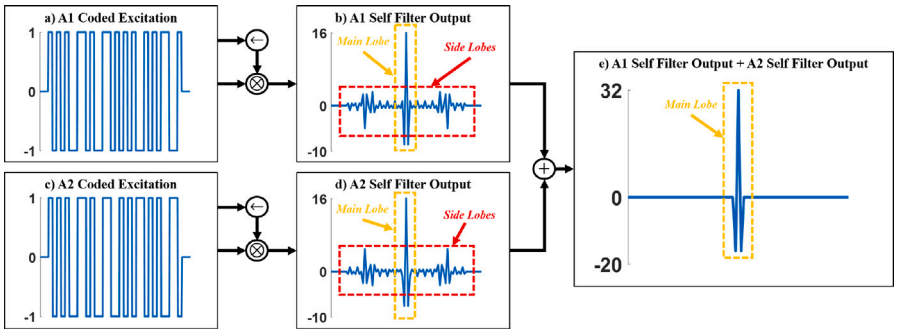


Fig. 3. The perfect Side Lobe cancellation when using Complementary Golay Sequence Coded Excitation with a sequence length $L = 16$: *(a)* Complementary Golay Sequence A1; *(b)* Sequence A2, the complement sequence of A1; *(c)* A1's filter response; *(d)* A2's filter response; and *(e)* summation of the two filter responses.

In the case of ultrasound NDE, prior research has often considered optimisation to be through the use of complementary sequence pairs, such as Complementary Golay Sequences (CGSs) [49]. CGSs make use of two separate measurements that result in SLs of similar position but opposite amplitude in their respective aperiodic auto-correlations, therefore allowing complete SL cancellation by summing each individual filter output from the dual-shot measurement — see Fig. 3 in which this process is shown. Further, a family of two sets of CGS pairs can be produced that are completely orthogonal through a similar process of producing opposing CLs in the cross-filter output [50].

Whilst the use of CGSs can indeed be considered optimal for some ultrasound NDE applications, the authors believe that alternative sequence types that can perform to a similar or greater degree than CGSs have not been considered due to the nature of how prior research has addressed the sequence optimisation problem. The majority of research into using coded excitation in ultrasound NDE has focused on how the technique can be used to improve a traditional inspection system's signal quality. Traditional inspection hardware typically utilises a high-voltage transmission architecture (high-voltage generation and high-speed high-voltage switching) combined with an isolated low-voltage reception architecture (analogue pre-amplification and optional analogue filtering before analogue-to-digital conversion). A simplified overview of such a system is shown in Fig. 4.

The traditional hardware setup is used such that a sufficiently high transmission energy can be delivered with narrow pulses with received information then amplified to fill the digitiser dynamic range such that a high baseline SNR and range resolution is achieved (i.e., the setup is designed to work without the need for coded excitation). However, when using this architecture, the transmission and reception events must be sequential (when using a pulse-echo probe configuration, as is the focus of this work). A staged transmit–receive process is required as the transmission amplitudes completely saturate the working range of the receiver components meaning no received information can be identified within the signal. Furthermore, the two sub-sets of components often require electrical isolation (transmit–receive switches) such that over-voltage related hardware failure of the receiver components is avoided, thus further mandating the use of staged transmit–receive events.

With hardware that uses sequential transmit–receive events, only short aperiodic sequences can be used to create coded excitation signals. (Aperiodic sequences here refers to sequences that require only linear convolution to achieve favourable compression

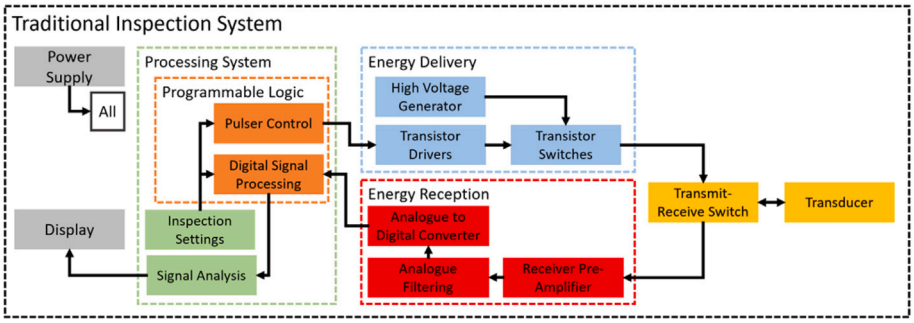


Fig. 4. The typical hardware components used in an ultrasound inspection system for non-destructive evaluation applications.

properties, periodic sequences and their use are covered later in Section 4.) The reasons for this are as follows. Firstly, with this hardware setup, the length of the signal dead-zone is directly matched to the length of the transmission signal, therefore short excitation signals must be used to avoid missing useful information. Secondly, aperiodic sequences must be used as only a single transmission event is possible before reception must begin. Attempting to use periodic sequences (either with multi-period transmission or extended matched filtering, both explained in Section 4) whilst also requiring a short single transmission event will result in multiple copies of received information being present in the final filtered signal. This will introduce severe signal distortion and make signal analysis greatly more complex.

With short aperiodic sequences mandated, the sequence design options are limited. The research into the use of periodic sequences, as has been shown in other applications, is not applicable, hence Barker and CGSs have remained the focus. Further, the limit on sequence length can make SNR gain minimal in some applications (e.g., contact transducer measurements without ultrasonic delay lines) in addition to restricting options for minimising SLs and CLs. Whilst these limitations do not inherently restrict coded excitation from being a useful technique to improve signal quality, CGSs can still allow some SNR gain without introducing any distortions and allow two-channel orthogonality, the authors believe that they can limit the usefulness of phase modulations as a technique, especially in low-power or large-channel MIMO applications. To overcome these limitations, the following section introduces an alternative hardware architecture that facilitates simultaneous transmission and reception. From this, we investigate if better sequence design is possible as a result of this change in acquisition strategy.

3. Low-power hardware for coded acquisitions

The previous section demonstrated that the traditional hardware architecture has issues relating to signal dead-zone, limited SNR gain and limited sequence type options when using coded excitations. Fundamentally, all of these issues arise as a result of the inability to simultaneously transmit and receive ultrasound signals through a single transducer element. This limitation is a result of the traditional system requiring high-voltage transmission amplitudes such that a high baseline SNR is still achieved when standard excitation pulses are used. To overcome this issue, the authors are proposing an adapted system for the use of coded excitations which removes the stated limitations of the traditional approach.

By dropping the excitation voltage to below the range over which the reception can occur, the receiver electronics can be directly coupled to the transmission electronics. Due to the superposition of signals, any received energy that returns while the transmission is active will add on to the transmission signal and still be digitised with this approach (providing the excitation voltage is sufficiently below the peak of the receiver range). Therefore, simultaneous transmission and reception can be achieved as post-processing (i.e., pulse-compression filtering) can isolate the transmitted and received components. Additionally, this approach has benefits as low voltage transmission is more easily achieved, thus the hardware complexity and cost of designing the ultrasound pulser is significantly reduced. Similarly, the receiver side electronics can also be simplified as pre-digitisation amplification is no longer needed (assuming the transmission electronics can be appropriately controlled to ensure the excitation voltages almost fill the receiver range).

This proposed hardware change will result in a significant performance drop when coded excitation signals are not used. The pre-filter noise floor (which we are assuming to be at the theoretical maximum for an ADC and therefore controlled by the digitisation resolution) will be proportional to the excitation signal instead of the expected echo amplitude. In other words, the maximum SNR of the pre-filter signal will be used up by the excitation signal itself as opposed to the echoes which contain the useful information. This is an issue as received information in ultrasound measurements is typically several orders of magnitude lower than the transmission signal (often 40 dB to 60 dB for piezoelectric transducers when using appropriate couplant). This is referred to as an *insertion loss* and arises due to phenomena such as beam spread, attenuation, scattering and large impedance mismatches at material boundaries. However, the ability to simultaneously transmit and receive information means that the signal dead-zone is no longer proportional to the length of the transmission signal, thus the hardware limitation on available sequence length for using coded excitation is removed.

The operating principle of using coded excitation on a low-power simultaneous transmission and reception capable platform is significantly different to how the traditional system operates. Fig. 5 compares the two approaches. With the traditional system, a

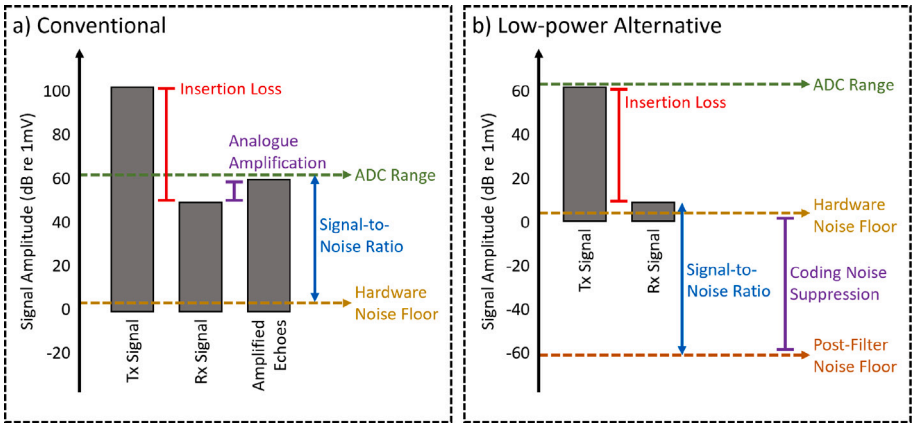


Fig. 5. Comparison of the two acquisition approaches. *(a)* the standard acquisition approach using high voltage transmission signals with receiver amplification to maximise the echo within the acquisition range. *(b)* our proposed alternative approach using low voltage transmission with echoes at the base of the acquisition range with coded excitation based pulse compression pushing the noise floor down to increase measurement SNR.

high-voltage transmission amplitude coupled with signal pre-amplification is used such that received information fills the dynamic range of the acquisition hardware, therefore enabling a high SNR relative to the hardware noise floor. Adding coded excitation to this platform allows for an increase in the energy of the received information such that the information stands further clear of this noise floor following matched filtering. With the alternative system proposed in this work, the received information will sit at, or even below, the hardware noise floor given the transmission amplitude is within the acquisition range. Adding codes to this system similarly increases the energy of the received information, however, the goal of the coded excitation is to now push down the post-filter noise floor relative to the excitation signal such that useful information is uncovered in the final signal. Whilst this achieves the same outcome regarding useful information SNR in the resulting timetrace, making the distinction is useful in understanding how this removes the limitation of the traditional approach. The traditional approach hits a barrier at which echo energy cannot be increased due to the need to stop transmitting and start receiving. With the alternative approach, the barrier at which the noise floor is pushed down is dictated not by the arrival of useful information but by the duration over which the total acquisition can last (which itself is determined by how long the environment of the measured system can be assumed to be stationary).

It is worth mentioning that we have assumed noise to be AWGN, however, in reality, noise is not necessarily white. Nonetheless, coded excitation inherently suppresses noise outside of the transmission bandwidth meaning the principle behind using ever increasing code lengths with the low-power approach holds in the presence of non-white noise, albeit with the potential for a reduction in compression performance should certain conditions be met (such as a DC offset in the noise introducing code breakdown). Even when considering noise frequencies within the transmission bandwidth, SNR gain will still occur when increasing code length as the filter searches not just for symbols of a set frequency but also of pre-determined symbol phase reversals, something noise is incredibly unlikely to mimic. There may be some noise conditions where the low-power approach drops in performance compared to the traditional system, but the authors are yet to come across such a condition.

To demonstrate the capability of this proposed alternative hardware architecture, experimental signals were recorded with the two acquisition systems shown in Fig. 6. Both systems were used to record pulse-echo measurements of a 10 mm mild steel block using a 5 MHz contact transducer (Olympus V109), also shown in Fig. 6. The first setup used a state-of-the-art conventional ultrasonic pulser and acquisition system (Peak NDT Ltd, MicroPulse LT2, Derby [51]) which was used to generate high quality reference signals to compare against. The LT2 was used with a 100 ns −200 V unipolar excitation signal (the system only supports unipolar excitations and thus cannot be tested with coded excitations), 15 dB gain of receiver amplification, and an analogue 5 MHz bandpass filter (3 dB limits of 3.70-6.40 MHz). Received signal digitisation used 12 bit resolution at a 50 MHz sample rate. The signal recorded from this setup is shown in the first row in Fig. 7. With the LT2 system, a minimum of $N = 2$ averaging must be used, hence the recorded signal has an SNR gain of roughly 3 dB over what would be achieved by a single shot with this hardware. The LT2 supports up to 70 dB receiver gain but only 15 dB was required to produce a first echo that filled the receiver dynamic range. The signal recorded with the LT2 using these settings is the highest quality possible from this hardware (without the use of additional digital signal processing techniques).

The second acquisition system used a Handyscope HS5-540XM which was controlled through a Matlab script. This allowed bipolar excitations via the high precision Arbitrary Function Generator (AFG) which has an output impedance of 50 Ω, therefore matching the approximate impedance of the V109 transducer. All excitation signals used with the HS5 AFG were created with a single cycle 5 MHz square wave, unless stated otherwise, thus effectively reducing the AFG to operate as a tri-state pulser only. The HS5 oscilloscope and AFG were both set to operate over a ±2 V range such that direct coupling between transmission and receiver components was possible via a simple T junction (when connected to an Olympus V109 transducer, the transmission voltage drops to approximately ±1.7 V due to the electrical characteristics of the transducer, oscilloscope and AFG, therefore the transmission

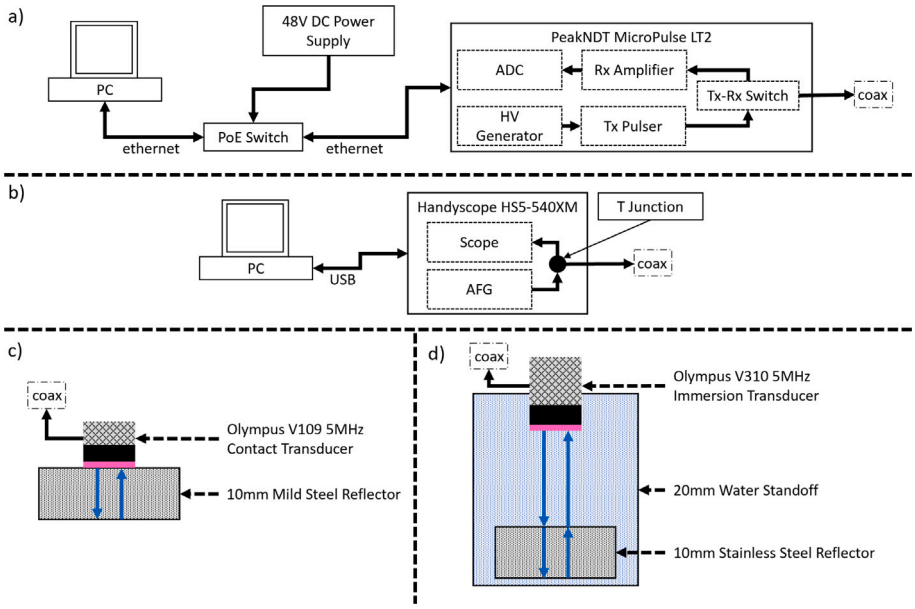


Fig. 6. The two acquisition systems used in this work when evaluating the use of coded excitation. *(a)* Experimental setup using a commercially available high voltage ultrasound acquisition system from PeakNDT. *(b)* Experimental setup using a USB function generator and oscilloscope. Both systems used to acquire signals for contact transducer *(c)* and immersion transducer *(d)* measurements.

amplitude could be set as equal to the receiver range without missing information). The oscilloscope was used in the DC coupling mode (meaning an input impedance of 1 MΩ/25 pF) and was operated with 14 bit precision at a 50 MHz sample rate (no receiver analogue amplification or filtering was used). A 14 bit precision is the default when initialising HS5 units, however, the results in the following would be largely unchanged if dropping the resolution to 12 bit as directly connecting the AFG and oscilloscope together results in a 55 dB noise floor, substantially higher than the noise imparted by least-significant-bit errors. Rows two to four in Fig. 7 show signals recorded with the HS5 with varying excitation parameters. Firstly, a standard excitation signal was used with $N = 100$ averaging. Following this, CGS based coded excitations were used with sequence lengths of $L = 8$, the longest CGSs that would be possible without the use of simultaneous transmission and reception given the early arrival of the first echo, and with $L = 4096$. All signals recorded on the HS5s were post-processed in Matlab to perform the necessary matched filtering. In Fig. 7, the first column shows the recorded signals on a linear scale normalised to the peak of the acquisition range. When CGSs are used, both recorded signals from the dual-shot measurement are shown. In the second column, post-matched filtered signals are shown on a log scale similarly normalised to the peak of the acquisition range such that the approximately 55 dB insertion loss can be seen when using the low-voltage architecture. The signal from the LT2 acquisition system was not matched filtered against a single symbol template given the signal already passed through an appropriate bandpass filter during reception.

To compare the signal quality from varying excitation parameters, the SNR for each filtered signal was calculated using Eq. (3). Eq. (3) compares the peak power from the first echo, taken as the square of the peak amplitude, V_{sig}, to the Root-Mean-Square (RMS) power of the signal in a position where no coherent information is expected, taken as the square of the RMS voltage within the same window, $V_{noise-RMS}$, which represents the additive power of the random noise. For the contact transducer measurements, the noise region was set as 10 μs wide (500 samples) starting at 300 μs such that all significant echo reverberations had died down. Each measurement was repeated at least 5 times with the mean SNR taken to mitigate the impact of random noise spikes impacting single measurements (more repetitions used for low SNR (≤20 dB) measurements to achieve greater stability). SNR is given on a log scale for easier comparisons.

$$SNR(dB) = 20 \times log_{10}\left(\frac{V_{sig}}{V_{noise-RMS}}\right) \tag{3}$$

The experimental signals shown in Fig. 7 demonstrate the effectiveness of using long sequences for low-power coded excitations, whilst also highlighting how traditional hardware can limit the usefulness of coded excitations. Despite using $N = 100$ averaging, the low-power hardware is only able to produce an SNR of 25.84 dB, lagging behind the conventional high-power system by almost 20 dB. Removing the expected 20 dB gain from using $N = 100$ averaging would result in even the highest amplitude echo sitting mostly within the noise floor. When applying the longest possible CGS pair that could be used if sequential transmit–receive events were required results in an SNR of only 18.55 dB, again significantly lagging behind the LT2 signal quality. This highlights how a limit on available sequence length can reduce the usefulness of coded excitation when used on systems with a poor baseline SNR. However, as the low-power system facilitates simultaneous transmission and reception, the system allowed the use of a sufficient

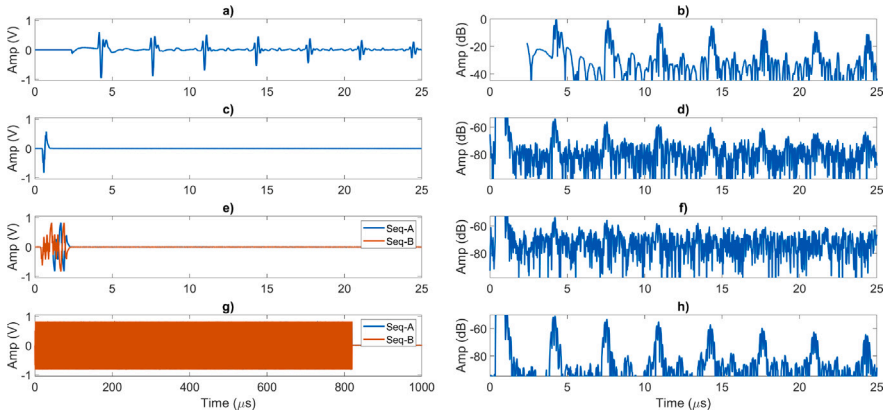


Fig. 7. First column: the signals recorded from the contact transducer experimental setup shown in Fig. 6 with varying excitation parameters on a linear scale normalised to the peak of respective system acquisition range. *(a)* LT2 acquisition system. *(c)* HS5 acquisition system without the use of coded excitation and with $N = 100$ averaging. *(e)* HS5 acquisition system with CGS $L = 8$ coded excitation. *(g)* HS5 acquisition system with CGS $L = 4096$ coded excitation. Second column: the post-matched filtered signals for the corresponding excitation parameters on a log scale similarly normalised to the peak of the respective system acquisition range. *(b)* SNR calculated as 44.50 dB. *(d)* SNR calculated as 25.84 dB. *(f)* SNR calculated as 18.55 dB. *(h)* SNR calculated as 44.56 dB.

sequence length ($L = 4096$ CGSs) such that it could match the SNR of the higher power LT2 system (approximately 44.5 dB for both) despite using simpler hardware.

From these results, the use of long sequences on a system capable of simultaneous transmission and reception has been shown to be a viable acquisition strategy for producing high quality signals with low-power transmissions. The superposition of signals and corresponding ML isolation following pulse compression results in no change to signal dead-zone when using increasing sequence lengths, thus allowing the SNR gain (shown by the results to follow the expected relationship of: $Gain_{SNR}(dB) = 10\times\log_{10}(L)$) from using codes to be increased as required such that the low-voltage system produces signals of appropriate quality (i.e., software-defined SNR). This makes the proposed architecture well suited to applications where only simple/low-power equipment is suitable. Examples of such applications are: permanently installed sensors for Structural Health Monitoring (SHM) or acquisition systems for medical wearables (a reduction in the number of components and in transmission amplitudes may make product certification easier and will likely allow for longer battery-life systems); low-cost large area coverage measurements (fewer acquisition components can reduce product cost and allow for more systems to be utilised); robotic applications (where lightweight, battery powered systems are often necessary); and university research (where cost is often the most important factor).

The drawback of using the proposed system is a reduced maximum PRF due to the use of long transmission signals. The LT2 measurement records an approximate 45 dB SNR from $N = 2$ measurement averaging. The max PRF that can be used in this application is 5 kHz (a 200 μs acquisition allows sufficient time for the echo reverberations to die down below the noise floor such that the next measurement can start) which is attainable by the LT2 (rated maximum of 20 kHz). Excluding data transfer time, the LT2 is achieving the 45 dB SNR in 400 μs. Setting the acquisition duration to 2000 μs for the low-voltage system allows the $L = 4096$ CGS pair excitation to be utilised which has been shown to match the signal quality of the LT2. Again excluding data transfer time as well as time taken to perform digital filtering, this has reduced the max PRF to 500 Hz. (A shorter $L = 1024$ CGS pair excitation can achieve approximately 39 dB SNR in 600 μs, almost matching the PRF of the LT2 without too substantial of a performance drop.) However, the proposed alternative approach presented here has additional benefits in how it can facilitate the use of alternative sequences which have not commonly been applied to coded excitation measurements. The following sections introduce unconventional sequences that have significant benefits in single- and multi-channel applications through pseudo-periodic and quasi-orthogonal ideal-like compression. Through such sequences, the drawback of a reduced PRF can be mitigated in MIMO applications by removing the need to operate channels sequentially.

4. Ternary odd-periodic (TOP) sequences

The previous section demonstrated the use of sequence lengths that resulted in excitation durations beyond the arrival of useful information whilst maintaining a pulse-echo measurement approach without missing/distorting information in the compressed output. This is shown to be possible due to the use of hardware that permits simultaneous transmission and reception. When utilising such sequence lengths on this low-voltage platform, periodic sequences can become advantageous despite previously being unsuitable for pulse-echo applications. To demonstrate this, an alternative sequence type, which we termed the Ternary Odd-Periodic (TOP) sequence, is introduced which can allow ideal-like compression from a single excitation event using extended matched filtering (pseudo-periodicity).

The sequences introduced in this work so far have produced favourable time domain compression properties when matched filtered using linear convolution (linearly convolved against the time reversal of themselves, referred to as the template). With linear convolution, the output is dependent on the multiplication and summation of sequence elements which are aligned with

elements in the template as the template slides across the sequence. When calculating the output for a shift/lag that results in elements aligning outside the width of the sequence, the outlying elements are ignored (equivalent to zero-padding such that outlying elements multiply to zero). Periodic pulse-compression works on the principle that circular convolution can instead be used such that period-overlap based summation can be utilised. With circular convolution, elements in the template that are outside the width of the sequence are modulo-L circularly shifted back to the start such that they are always present during the multiplication and summation steps. With circular convolution, period-overlap based cancellation can aid in suppressing SLs and producing more favourable compression properties.

In the context of active ranging, periodic sequences can be used either via cyclic convolution of received signals or via multi-period transmission or extended matched filtering. Cyclic convolution requires both the received signal and the template have the correct number of samples in such that modulo-L circular shifting produces correct alignment. Such requirements on acquisition duration and alignment are hard to fulfil, hence why alternative options exist. Both alternative options utilise the fact that cyclic convolution can be recreated with linear convolution providing multiple periods of the original sequence are present during the convolution operation. With multi-period transmission, multiple periods of the periodic coded excitation are transmitted sequentially such that a template containing a single period of the coded excitation can be used with linear convolution to achieve the pulse compression. With extended matched filtering, the opposite occurs; a single period of the coded excitation is transmitted and the template used to filter against contains multiple periods instead. In both options, the output from the filtering process contains the output that would be achieved from an ideal cyclic convolution. For more detail on the comparison between aperiodic and periodic pulse compression signals, refer to the explanation given in [10].

A well known example of a periodic sequence is the Maximum-Length-Sequence (MLS) [52,53]. With cyclic convolution (or equivalent), MLSs produce a high intensity ML surrounded by a unity DC-offset. This is similar to achieving complete SL suppression, but when band-limited symbols are used, the DC-offset turns into a train of low intensity SLs which set the post-filter noise floor. To achieve sufficiently low SLs with MLSs such that a high SNR signal can be produced with the proposed low-power architecture, a sequence length of $L = 65536$ would be required with MLSs to theoretically achieve a near 40 dB SNR when insertion losses are at 55 dB. To avoid the need for such large sequence lengths, the authors are instead using the sequences introduced in [54] to demonstrate the effectiveness of using periodic sequences on the proposed low-power platform.

The sequences introduced in [54], which we are referring to as Ternary-Odd-Periodic (TOP) sequences, are produced using Galois finite field mathematics, similar to the foundation behind which MLSs are produced. In [54], the Legendre symbol is used to convert elements from an odd-prime extended Galois field (which allows vast flexibility in picking an appropriate sequence length, admittedly at the cost of high calculation complexity) into a ternary sequence through a specific equation. These sequences differ to MLSs in that they use odd-periodicity and a ternary alphabet, both of which are explained in the following.

When using binary sequences to create coded excitations, each sequence value sets a complete reversal of symbol phase. For ternary sequences comprised of $+1$, -1, and 0, each sequence value represents either a complete symbol phase reversal ($+1$ being positive start phase, -1 being negative start phase) or a complete symbol cancellation (0 represents a zero-energy symbol). This can be considered as introducing a basic amplitude modulation (on and off) into the phase modulation. Ternary sequences are as simple to transmit as binary sequences, however, they introduce a reduction in SNR gain compared to standard binary sequences due to part of the excitation duration spent transmitting zero energy. The sequences from [54] achieve the highest possible energy efficiency for a ternary alphabet sequence, though, given each sequence contains only a single element that is 0.

Odd-periodicity refers to the need for alternating copies of the sequence in the signal that contains multiple periods (either transmission or template) to be sign inverted before entering the convolution stage. MLSs and other periodic sequences rely on the cyclic shifting of sequence elements to achieve the SL suppression. TOP sequences require that the elements that are cyclically shifted are first sign inverted such that complete SL cancellation is achieved. For multi-period transmission, each sequential period needs to be inverted. For extended matched filtering, the template must be made with odd copies of the period being sign inverted.

The reason the authors have decided to focus on the use of TOP sequences is shown in Fig. 8. TOP sequences exhibit poor aperiodic and periodic compression properties, as shown in rows one and two. In row three, the template used to filter the original sequence against contains the time reversal of three copies of the original sequence with copies one and three sign inverted. The output from this filter operation contains three MLs which correspond to when the original sequence aligns with each sequence period in the template. In between the end MLs, in the region we have termed the central period, there is complete SL cancellation surrounding the central ML. This output would also be achieved if the template contained a single period which was used to filter against three periods of the sequence with alternating period sign inverted (equivalent to the previously mentioned multi-period transmission). However, the authors are focusing on the use of extended matched filtering as this is preferential in reducing acquisition time given the need to transmit only a single instance of the coded excitation. For completeness, it is worth highlighting that the extended matched filter requires three periods to achieve a true ideal central period. Two periods results in ideal compression on only one side of each ML which results in SL distortions if multiple reflected echoes are present. Greater than three periods can be used but are not required. The central period containing complete SL cancellation also holds true when a band-limited symbol is introduced, as is shown in row four.

It can now be understood how the use of TOP sequences can work well when combined with the proposed low-power hardware platform from Section 3. Extended matched filtering of a single copy of a TOP sequence produces ideal compression within the central period. Setting the width of the central period to extend beyond the duration of the impulse response of the medium under test (the duration over which echoes of significant amplitude are still returning) in an ultrasonic inspection allows a single TOP-sequence excitation event to produce perfect compression for all reflected echoes. TOP sequences can therefore remove the need to use dual-shot CGSs to achieve ideal compression within the region of interest for an ultrasonic inspection, something that has

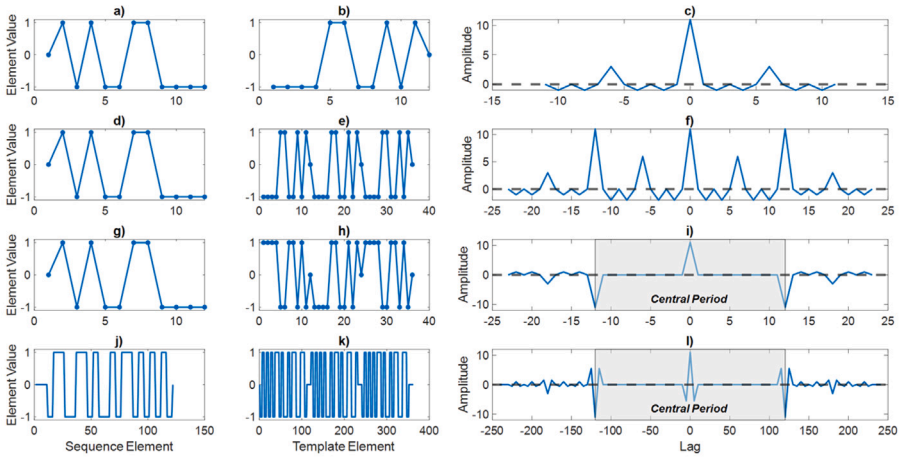


Fig. 8. TOP sequences filtered against varying templates. *(a)* $L = 12$ TOP. *(b)* Flipped $L = 12$ TOP. *(c)* sequence in *(a)* $\otimes$ template in *(b)*. *(d)* $L = 12$ TOP. *(e)* Flipped three consecutive copies of $L = 12$ TOP. *(f)* sequence in *(d)* $\otimes$ template in *(e)*. *(g)* $L = 12$ TOP. *(h)* Flipped three copies of $L = 12$ TOP with alternating copies sign inverted. *(i)* sequence in *(g)* $\otimes$ template in *(h)*. *(j)* sequence in *(j)* up-sampled and convolved with a single cycle square symbol. *(j)* template in *(h)* up-sampled and convolved with a single cycle square symbol. *(l)* signal in *(j)* $\otimes$ template in *(k)*. The central period, which extends from $-(L-1)$ to $+(L-1)$ (where L is the sequence/signal length) and contains ideal side lobe cancellation throughout, is highlighted in *(i)* and *(l)*.

not been shown in previous work. The use of TOP sequences mandates the use of the proposed low-power hardware architecture, though, as the transmission duration must exceed the duration of the medium under test's impulse response, something not possible when using a traditional hardware architecture in a pulse-echo application, as has been previously explained.

An important note on the use of TOP sequences with extended matched filtering: the use of multiple sequence periods to produce the filter template changes the relationship between SNR and sequence length. With aperiodic sequences, SNR gain over an uncoded (but appropriately matched filtered) measurement is directly proportional to the sequence length, L, as this controls the increase in transmitted energy. During the filtering process, there will be a point where all L individual bursts sum together. Therefore, the useful information amplifies to L times its original value giving an increase in useful power of L^2 compared to a standard un-coded measurement. When filtering signals against coded excitations (either fully matched or sequence only filters), each post-filter value contains the sum of L (more) noise points in the pre-filter signal. This corresponds to an increase in noise power of L giving a resulting total SNR gain of L by itself.

With extended matched filters used to enable pseudo-periodicity, there will still be a point of alignment that results in L individual symbols summing together, but there will now be an additional E times more points summed together to produce each post-filter value compared to a standard matched filter, where E is the number of sequence copies used to produce the template. This results in an increase in noise power in the post-filtered signal thus meaning the SNR gain from using periodic coded excitation is not a one-to-one linear relationship with sequence length. Instead, the SNR gain from using periodic codes is proportional to the sequence length and the total acquisition time beyond the end of the transmission. If the acquisition duration is set identical to the excitation period, then there can only be L total noise points which can enter the summation, thus ensuring an L gain in SNR. However, the record length for ultrasound measurements, denoted here as R, must be set as longer than the transmission duration, denoted as T, to account for the time of flight for each symbol returning from each reflector. Incorrect compression will occur if a complete sequence of symbols is not recorded for each reflector.

The additional reception time therefore allows for an increased number of noise points to enter the signal which impacts each post-filter value given the extended matched filter requires summations of multiple transmission periods worth of samples. Still assuming noise is AWGN, the noise power gain as a result of using an extended matched filter is proportional to L plus the total number of additional samples in the recorded signal divided by the symbol width, denoted as W. This results in the following relation for expected SNR gain:

$$Gain = \begin{cases} \frac{L^2}{L+\frac{R-T}{W}}, & \text{if} R \leq 2 \times T \\ \frac{L^2}{2 \times L}, & \text{otherwise} \end{cases} \tag{4}$$

The symbol width plays a factor in Eq. (4) as this determines how many additional sequence elements relate to a given additional reception duration. Once the additional reception period exceeds the duration of the transmission period, no further reduction in SNR gain will be noted given the additional noise points will exist beyond two transmission periods and therefore have no impact on the summations within the first compression period. For completeness, the SNR gain would instead reduce to a minimum $\frac{L}{3}$ relationship if a transmission periods worth of data is recorded before the start of the transmission signal, though this is never necessary. Given this relationship between sequence length and gain, the optimal excitation signal based on periodic sequences may utilise a longer symbol to increase noise suppression (and in some cases transduction efficiency) with a shorter sequence length.

Multi-period transmission does not suffer from this reduced SNR gain relationship with sequence length; however, it increases acquisition duration substantially and reduces SNR gain relative to total transmitted energy given only a single period will sum together when filtered against a standard matched filter, thus extended matched filtering is still the preferred option in this work.

In the following section, families of quasi-orthogonal sequences are created based on further utilising the ideal-like compression in the central period from TOP sequence extended matched filtering. To first see the validation of the use of TOP sequences in an aperiodic fashion for producing high quality signals, see Section 6.1.

5. Circularly shifted (-CS) sequence families

The previous section introduced TOP sequences which achieve ideal compression within a set central period following extended matched filtering. The central period contains no SLs and extends for the length of the sequence itself. Based on these properties, TOP sequences can be used as the foundation for producing a family of quasi-orthogonal sequences by using what we are referring to as a Circularly-Shifting production method, denoted as -CS.

Orthogonality, as previously explained, is the concept of sequences that cancel to zero when cross-filtered against each other. Whilst TOP sequences (or any other binary/ternary sequence) cannot be extended to produce true-orthogonality for a large sequence family, quasi-orthogonality can instead be achieved. Quasi-orthogonality refers to the concept of sequences that only produce regions of complete cancellation following cross-filtering. Setting this region, which we have termed the orthogonal zone, to extend across the duration of interest in an ultrasonic signal allows for complete removal of crosstalk across channels in a MIMO application without requiring truly orthogonal sequences.

Given TOP sequences inherently have zero correlation with time-lagged versions of themselves when extended matched filtering is used, it must hold true that a new sequence that is itself a circularly-shifted version of the original sequence would have no correlation with the original over the number of lags it has been shifted by. From this principle, an original TOP sequence of length L can produce $L-1$ additional sequences that are all time-lagged by 1 shift (see the Conference Matrix introduced in [54]). It is important to note here that the circular shifting must also have sign inversion given TOP sequences require odd-periodicity for achieving SL cancellation in the perfect central period. Each sequence in this family will have its own perfect central period following extended matched filtering. In addition, each sequence when extended cross-filtered against each other sequence will have zero in the central lag. This principle can be adapted to become of use in MIMO active ranging applications. To do so, the following steps are taken:

First: define a region of interest for each channel which will become the duration by which CLs will be shifted — the length of the orthogonal zone. This will become the length of the timetrace that contains no CLs. Convert this timetrace length into the required number of symbols to fill such a duration. Call this K which will become the shift amount.

Second: define the number of codes in the family that need to be made. This is the number of channels in the MIMO application that will be used simultaneously. Call this M.

Third: multiply K by M to find the required length of the first sequence to be made ($L_{required} = K \times M$). This first sequence, which we will term the primer, will be produced using the standard method mentioned in [54]. The actual sequence length will become the next prime number above $L_{required}$ plus one.

Fourth: generate the base primer, S_0. Depending on the choice of field extension factor or prime number, this step will be computationally intensive, but only needs to be performed once.

Fifth: circularly shift the primer sequence by K elements. Each element that is circularly shifted must have its sign inverted (0 stays as 0). The new sequence produced will be S_1. Repeat this step with increasing shift amounts to produce all members of the family.

Sequence families produced using this methodology do not require element cancellation to achieve quasi-orthogonality, as would be the case when using traditional orthogonal sequences (such as orthogonal pairs of CGSs) or more common quasi-orthogonal sequences such as Zero-Correlation-Zone (ZCZ) sequences [55–57]. Instead, standard MLs are produced but in a shifted position such that they do not impact the region of interest. Therefore, without requiring element cancellation that can be subject to breakdown, a family that behaves perfectly orthogonal within a set region of interest can be produced. A TOP-CS quasi-orthogonal family produced using this methodology is shown in Fig. 9. It is important to note that quasi-orthogonality is only exhibited if each transmission event starts at the same time as time-shifting can also be introduced through delaying transmissions across channels. The need for simultaneous transmission events across channels is the reason that -CS quasi-orthogonal families have minimal use in telecommunications when crosstalk can arrive at unexpected intervals.

In the context of MIMO ultrasonic applications, TOP-CS sequence families can be used such that each individual channel is assigned its own excitation signal that allows it to operate independently without concern of crosstalk. Each channel's transmission signal will produce zero SLs following extended matched filtering against its own template, as is expected when using TOP based coded excitations. When channels are operated simultaneously, ultrasonic crosstalk present in the recorded signals will be shifted away by the duration of the orthogonal zone during filtering. By ensuring the orthogonal zone duration is sufficient such that it extends beyond the arrival time of all significant crosstalk echoes (those above the noise floor), all ultrasonic crosstalk will automatically be removed from the region of interest in the post-filter signals, thus perfect SL and CL suppression within the set region is achieved. Cross-filtering the received signal from any channel with the template associated with another channel's transmission then allows for information that has passed between the two channels to be identified and isolated, again with other ultrasonic energy automatically shifted away from the region of interest.

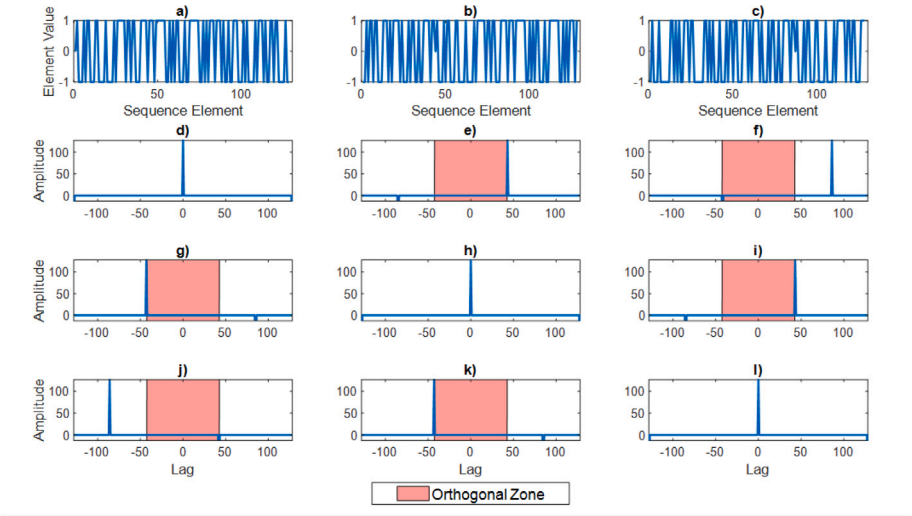


Fig. 9. The matrix of correlations when using TOP-CS sequence families with $K = 40$ and $M = 3$, leading to $L = 128$. *(a–c)* sequences 1, 2 and 3 respectively. *(d–f)* sequence 1 extended matched filtered against sequences 1, 2 and 3 respectively. *(g–i)* sequence 2 extended matched filtered against sequences 1, 2 and 3 respectively. *(j–l)* sequence 3 extended matched filtered against sequences 1, 2 and 3 respectively. Crosstalk free orthogonal zone in cross-filtered signals, calculated as sequence length divided by total family size, shown in each extended matched filter output.

Important points to note before continuing: first, if the length of the orthogonal zone is too short relative to the length of the ultrasonic impulse response of the physical system, typically low-amplitude CLs will remain which relate to late-arriving echoes. The remaining CLs in this scenario may or may not be acceptable depending on the application's need for an increased PRF versus complete artefact removal. Second, the crosstalk shifting based isolation described here works only on ultrasonic energy (i.e., energy that propagated between channels). Electronic crosstalk will not be shifted away as electronic crosstalk results in small copies of the transmission signal from neighbouring channels being transmitted on each other which results in propagated energy that cannot be isolated.

In the previous section, the main drawback associated with the proposed low-voltage system using long sequences is the increase in acquisition time required. In the context of MIMO applications, systems using traditional high-voltage excitations must sequentially operate measurement channels such that distortions relating to ultrasonic crosstalk are avoided. This increases the acquisition time for the total MIMO system as it becomes the multiple between number of channels and max PRF available for the specific application (i.e., 200 μs for the contact transducer application in earlier sections would require 800 μs for complete measurements on 4 channels). When using TOP-CS coded excitations, all channels in the MIMO setup can operate simultaneously given crosstalk is removed in post-processing. Setting the region of interest to be 200 μs for the contact application and using a family size of 4 channels results in each acquisition taking 1000 μs (800 μs transmission signal plus 200 μs of post-transmission reception). Therefore, there is a less significant reduction in total system PRF when using the proposed alternative setup than in the single-channel application. The difference between total system PRF for uncoded sequential and simultaneous coded TOP-CS setups becomes negligible as the number of channels increases. In the following section, experimental signals are recorded to validate the claims made about the use of TOP and TOP-CS sequences in ultrasound applications. Specifically in Section 6.2, a multi-channel ultrasound setup is used to highlight the capabilities of using TOP-CS on a low-voltage architecture.

6. Experimental validation

The previous sections introduced the use of alternative sequences that achieve quasi-ideal compression and quasi-orthogonality via extended matched filtering. The following experimental results are used to validate that aperiodic applications of such sequences can allow for the production of high quality signals without filter artefacts when used on the proposed low-power architecture from Section 3. This section is separated to show results to highlight SNR improvement for a single-channel setup (Section 6.1) and to show crosstalk suppression in a multi-channel application (Section 6.2).

6.1. Single-channel applications

This section first uses the contact transducer experimental platform (first introduced in Section 3) to validate that aperiodic applications of TOP sequences on a low-power platform can produce high SNR pulse-echo signals without filter artefacts. Additional validation is then achieved by recording immersion pulse-echo signals with varying excitation parameters such that SNR versus acquisition duration and total excitation energy can be plotted.

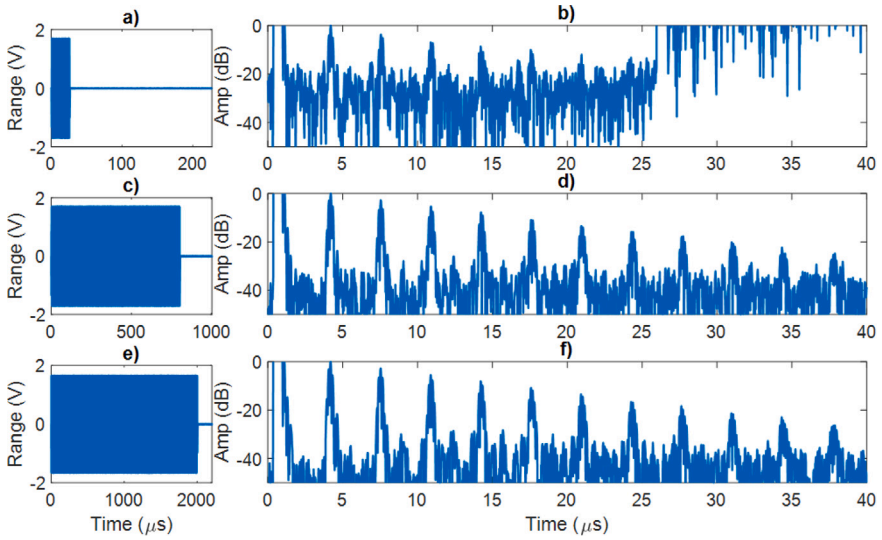


Fig. 10. Signals recorded using the low-voltage architecture with varying length TOP sequences on the contact transducer application shown in Fig. 6. *(a)* recorded signal with TOP $L = 128$ on a linear scale over the acquisition range. *(b)* signal from plot *a* on a log scale normalised to the first echo — SNR not calculated due to periodic overlap. *(c)* recorded signal with TOP $L = 4002$ on a linear scale over the acquisition range. *(d)* signal from plot *c* on a log scale normalised to the first echo — SNR calculated as 40.85 dB. *(e)* recorded signal with TOP $L = 10008$ on a linear scale over the acquisition range. *(f)* signal from plot *e* on a log scale normalised to the first echo — SNR calculated as 45.29 dB.

Firstly, Fig. 10 shows A-scans of increasing signal quality due to the use of increasing length TOP sequences. The first row highlights the need for the excitation signal's period (controlled by the sequence length) to exceed the duration over which useful information is recorded. An excitation period of 25 μs is used in this plot ($L = 128$ sequence) which introduces significant distortion to the low SNR signal. As previously explained, when using pseudo-periodicity, each ML in the final signal will have corresponding ML-periods (and out-of-window SLs) placed a period-width away, so this period must be of sufficient length such that the lobe copies do not introduce coherent noise which complicates analysis. Contrary to the traditional architecture which has a maximum allowable excitation duration, with pseudo-periodicity there is instead a minimum excitation duration for producing useful signals.

In the second row of Fig. 10, the excitation period is sufficient ($L = 4002$ sequence) such that distortion does not occur while enabling a 1 kHz PRF. This results in an SNR of 40.85 dB, thus producing high quality signals without requiring impractical acquisition durations. Further increasing the acquisition duration to 2.2 ms (454 Hz PRF) allows a sequence length of $L = 10008$ which produces an SNR of 45.29 dB and matches the performance of the LT2 system — this is shown in the third row.

To validate the performance gain with varying excitation parameters, repeat measurements were recorded such that a trend between SNR and excitation energy and acquisition duration could be plotted. To mitigate the impact of couplant conditions on a contact transducer varying with time and to provide a higher baseline SNR to compare against, an immersion experimental platform was used, also shown in Fig. 6. For the immersion platform, the LT2 and HS5 acquisition systems were used with a 6.35 mm unfocused immersion transducer (Olympus V310) placed in a water tank 20 mm from the front surface of a 10 mm stainless steel reflector. Example signals from this setup are shown in Fig. 11. All SNR results were calculated using the front wall entry echo and with a noise region set at 300 μs (sufficiently after all echoes had decayed). The LT2 system recorded signals without receiver amplification and using −100 V to −200 V excitation amplitudes (similar receiver filtering and digitisation parameters were used as the contact application). The −200 V excitation on the LT2 produced a front wall echo of sufficient amplitude as to fill the receiver dynamic range, hence no receiver amplification was used. The HS5 was used with ±1.9 V peak transmission amplitudes with a ±2 V receiver range. To account for the different electrical characteristics of the immersion transducer, the transmission amplitude had to be dropped to below the peak of acquisition range to ensure no information was missed when using long sequences. The HS5 recorded signals with and without coded excitations of varying type and length in addition to other varying excitation parameters for performance comparison purposes. TOP sequence acquisitions were repeated with an acquisition duration of the transmission duration plus 300 μs, the minimum required to ensure perfect compression such that distortions did not impact SNR calculations, and plus an additional 500 μs and 1000 μs to verify the impact of excess noise points impacting SNR gain.

Fig. 12 shows the change in SNR with excitation energy and required acquisition duration as excitation parameters are changed on the immersion setup. In each figure, the SNR from the LT2 using −100 V and −200 V excitation amplitudes are shown to reference the performance of industry standard equipment. The required excitation duration is calculated as the total length of the excitation plus 300 μs, the minimum time required for echo reverberations to fall below the noise floor, then rounded to the nearest 25 μs. Excitation energy is calculated as the relative increase from a standard single symbol (1-cycle square wave) ±1.9 V excitation signal (i.e., increases with sequence length/total number of symbols and increases with the square of an amplitude increase). Table 1 provides all results.

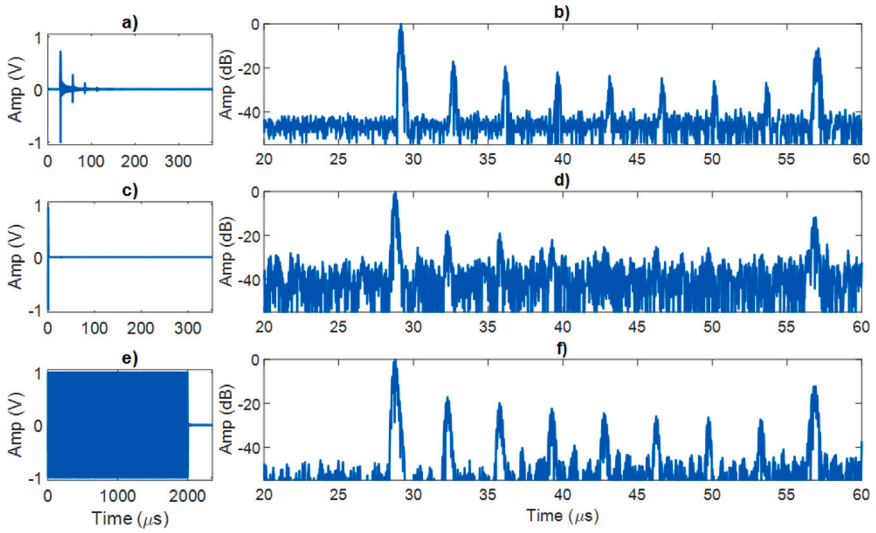


Fig. 11. Recorded signals from the immersed transducer application, shown in Fig. 6, normalised to the peak of the acquisition range on a linear scale (*left*) and on a log scale (*right*). *(a–b)* signal from the LT2 acquisition system using a −200 V excitation. *(c–d)* signal from the low-voltage HS5 acquisition system without using coded excitation with $N = 100$ averages. *(e–f)* signal from the low-voltage HS5 acquisition system using TOP $L = 4002$ coded excitation.

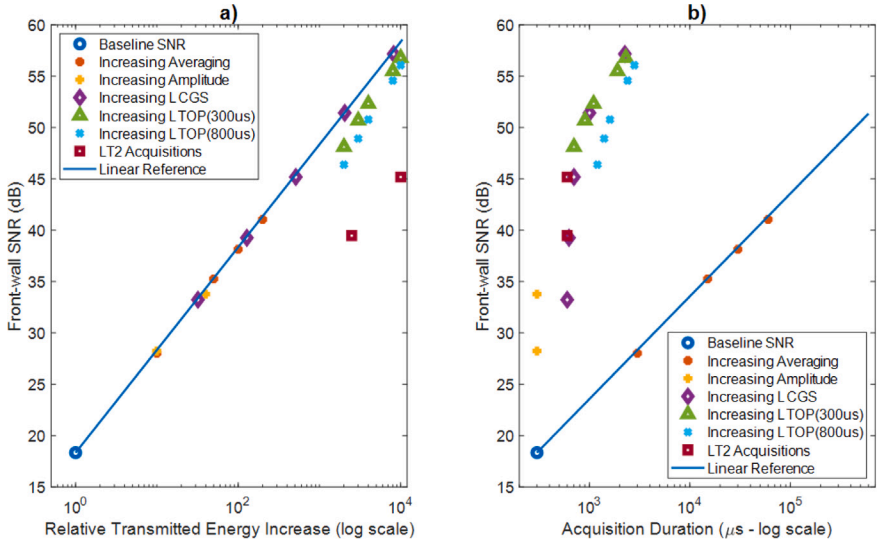


Fig. 12. The change in SNR with: *(a)* a relative increase in transmitted excitation energy; and *(b)* a change in total acquisition duration. In both plots, a linear reference that follows the theoretical performance of using measurement averaging is shown. Results are shown for TOP sequence measurements with a total acquisition duration of the transmission length plus 300 μs (TOP(300us) in the legend) and the transmission length plus 800 μs (TOP(800us) in the legend).

Overall, the results verify that TOP sequences matched filtered against multiple, alternately phase reversed copies of themselves can be used effectively in producing artefact free high quality ultrasound pulse-echo signals from single element transducers and from a single excitation event. The use of an extended matched filter reduces the SNR gain to a fractional linear relationship meaning TOP sequences lag behind CGSs for the same total number of symbols. Nonetheless, the removal of the need for two separate excitations (and the need to wait for reverberations to die down between them) can allow TOP sequences to achieve similar or greater SNR performance as CGSs for a given acquisition duration.

Both optimised aperiodic and pseudo-periodic sequences are shown by the results to be very effective tools when combined with low-power hardware which facilitates simultaneous transmission and reception. Utilising codes on a low-power platform therefore makes it possible to match the performance of commercial grade high voltage ultrasound acquisition systems with a reduced hardware complexity. With the immersion setup as an example, TOP sequences on the low-power platform can produce a greater front-wall SNR than the LT2 whilst enabling a ≥ 1 kHz PRF.

Table 1
Results from using varying excitation parameters on the immersion experimental setup. TOP sequence results are shown for varying acquisition durations, denoted as TOP-Xus for an acquisition duration of the transmission length plus X μs.

Excitation Type	Peak Pulser Amplitude	Sequence Length	Number of Averages	Total Number of Symbols	Relative Energy Increase	Front-wall SNR (dB)	Minimum Acquisition Duration (us)	Expected Front-wall SNR (dB)
Standard	1.9	1	1	1	–	18.34	300	–
Standard	1.9	1	10	10	10	28.02	3000	28.34
Standard	1.9	1	50	50	50	35.26	15 000	35.33
Standard	1.9	1	100	100	100	38.14	30 000	38.34
Standard	1.9	1	200	200	200	41.05	60 000	41.35
Standard	6	1	1	1	9	28.24	300	28.33
Standard	12	1	1	1	36	33.77	300	34.35
CGS	6	16	1	32	288	43.09	600	43.38
CGS	1.9	16	1	32	32	33.23	600	33.39
CGS	1.9	64	1	128	128	39.26	625	39.41
CGS	1.9	256	1	512	512	45.18	700	45.43
CGS	1.9	1024	1	2048	2048	51.42	1000	51.45
CGS	1.9	4096	1	8192	8192	57.16	2250	57.47
TOP-300us	1.9	2004	1	2004	2004	48.11	700	48.94
TOP-300us	1.9	3002	1	3002	3002	50.68	900	51.36
TOP-300us	1.9	4002	1	4002	4002	52.31	1100	52.98
TOP-300us	1.9	8010	1	8010	8010	55.48	1900	56.64
TOP-300us	1.9	10 008	1	10 008	10 008	56.77	2300	57.74
TOP-800us	1.9	2004	1	4002	4002	46.38	1100	46.60
TOP-800us	1.9	3002	1	8010	8010	48.92	1900	49.44
TOP-800us	1.9	4002	1	4002	4002	50.77	1100	51.35
TOP-800us	1.9	8010	1	8010	8010	54.57	1900	55.62
TOP-800us	1.9	10 008	1	10 008	10 008	56.07	2300	56.89
TOP-1300us	1.9	2004	1	4002	4002	46.36	1100	45.08
TOP-1300us	1.9	3002	1	8010	8010	48.67	1900	48.11
TOP-1300us	1.9	4002	1	4002	4002	50.1	1100	50.17
TOP-1300us	1.9	8010	1	8010	8010	54.01	1900	54.80
TOP-1300us	1.9	10 008	1	10 008	10 008	55.45	2300	56.17
LT2	100	1	2	2	2770	39.46	600	–
LT2	200	1	2	2	11 080	45.17	600	–

The experimental demonstrations have shown that this approach works well for standard piezo-electric transducers with an insertion loss between 40 dB and 60 dB. However, the range of applicability of this approach is somewhat limited to systems that have an insertion loss of a similar order. This technique simply pushes the noise floor down relative to the excitation signal meaning there is a limit to how far one can go within reasonable acquisition times over which the system remains stationary, which is the fundamental assumption that is made when employing this methodology. Electromagnetic Acoustic Transducers (EMATs) or air couple transducers can have insertion losses in excess of 100 dB thus making them unsuitable for using this methodology (unless material control can be used to ensure system stationarity).

6.2. Multi-channel applications

Having demonstrated the ability to use TOP sequences aperiodically in producing high SNR measurements, the following looks to validate the use of TOP-CS families in achieving crosstalk suppression in MIMO applications via quasi-orthogonality. The experimental setup used to achieve this is shown in Fig. 15.

As can be seen in Fig. 15, a 2-facing-2 configuration of contact transducers (all Olympus V109 5 MHz transducers) was used to create the MIMO application. Each transducer was connected to a Handyscope HS5 with all 4 HS5s controlled through a single Matlab script. The HS5s connected to V109-2, V109-3 and V109-4 used the external trigger from the HS5 connected to V109-1 to start their respective acquisitions such that transmission signals were appropriately aligned. Whilst the 2-facing-2 grid is not a common MIMO configuration used in ultrasonic inspections (as opposed to parallel transducers or phased arrays), it was used for this demonstration as it allowed for large-scale controlled crosstalk to be introduced by creating pitch-catch propagation paths. When operating each transducer simultaneously, each channel records its own standard pulse-echo thickness measurement. Due to the positioning and size of each transducer as well as natural beam spread, multiple pitch-catch ultrasound paths are present in this MIMO setup, hence the introduction of large controlled crosstalk at predictable arrival times. Further, using the 2-facing-2 configuration allowed for the HS5s to be used with coax connected transducers, thus allowing the setup to test the ability to suppress ultrasonic crosstalk without concern of electronic crosstalk distortions.

When operating the four channels in the 2-facing-2 configuration simultaneously without the use of coded excitation, the signals shown in the left column of Fig. 14 are recorded. To acquire these signals with sufficient SNR from a standard excitation pulse, the HS5s were operated with a transmission amplitude of ±12 V and a reception range of ±0.2 V so as to approximate a more conventional system. As shown in Fig. 14, each recorded signal contains prominent pulse-echo and pitch-catch echoes, therefore highlighting the severity of the crosstalk across channels.

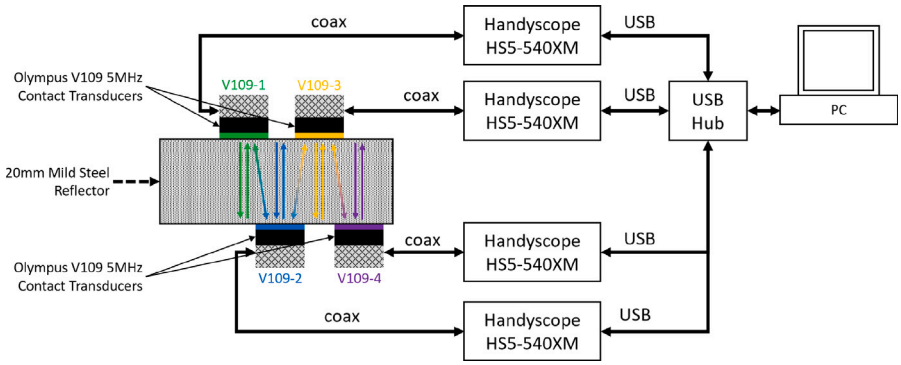


Fig. 13. Multi-channel experimental setup using 4 low-voltage Handyscope HS5s to perform acquisitions on 4 contact transducers with a 2-facing-2 configuration as to introduce controlled pitch-catch crosstalk.

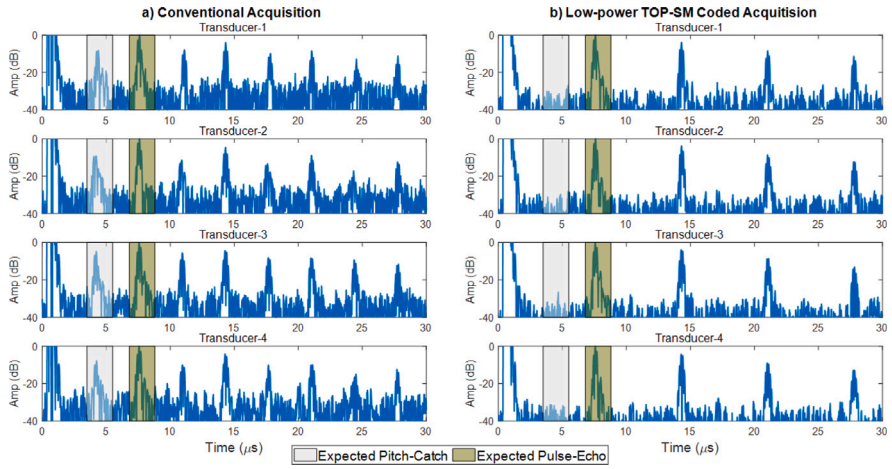


Fig. 14. Pulse-echo response measured on transducers facing each other (as shown in Fig. 13). *(a)* using uncoded excitation signals with ±12 V transmission amplitudes. *(b)* using TOP-CS $L = 4002$ $M = 4$ coded excitations with ±2 V transmission amplitudes. All signals shown on a dB scale normalised to the peak of their respective first pulse-echo echoes.

Reducing each HS5's AFG to a ±2 V transmission amplitude and increasing the reception range to ±2 V allowed for TOP-CS coded excitations to be applied. Using $L = 4002$ TOP-CS sequences with a family of $M = 4$ (giving an approximately 200 μs orthogonal zone, sufficient for this application) produced the signals shown in the right column of Fig. 14. To produce these signals, each of the recorded signals from each transducer was extended matched filtered against their own transmission signal, thus allowing complete isolation of just the pulse-echo echoes without any pitch-catch crosstalk. Further extended matched filtering each of the received signals against each of the other transmission signals allowed for the full matrix of A-scan data to be uncovered despite using only a single transmission event. The full matrix of data can be seen in Fig. 15. In the array of data, the pitch-catch echoes from neighbouring channels can further be identified and separated from each other.

The multi-channel experimental demonstration shown here has verified that the use of TOP-CS based coded excitations can allow for the complete removal of crosstalk across transducers in the set orthogonal zone. By allowing the simultaneous operation of multiple measurement channels, low-power systems utilising TOP-CS sequences can match the signal quality of traditional high-voltage systems and near-match the total system PRF.

7. Conclusions

In this work, we have pointed out how a traditional hardware architecture imposes limitations on how coded excitation can be applied in ultrasound measurements. The requirement to finish transmitting energy before reception can take place, as is imposed by using high voltage transmissions, results in a limit to the gain that can be achieved by increasing sequence length. Furthermore, the need to use aperiodic sequences limits the options available for minimising SLs and CLs, effectively leaving CGSs as the only solution. To overcome these issues, we present an alternative hardware architecture that is designed around the assumption that coded excitation will be used. By avoiding the need to achieve a high baseline SNR, low-voltage excitations can be employed which facilitates the simultaneous transmission and reception of ultrasonic signals on a single transducer element. With the excitation

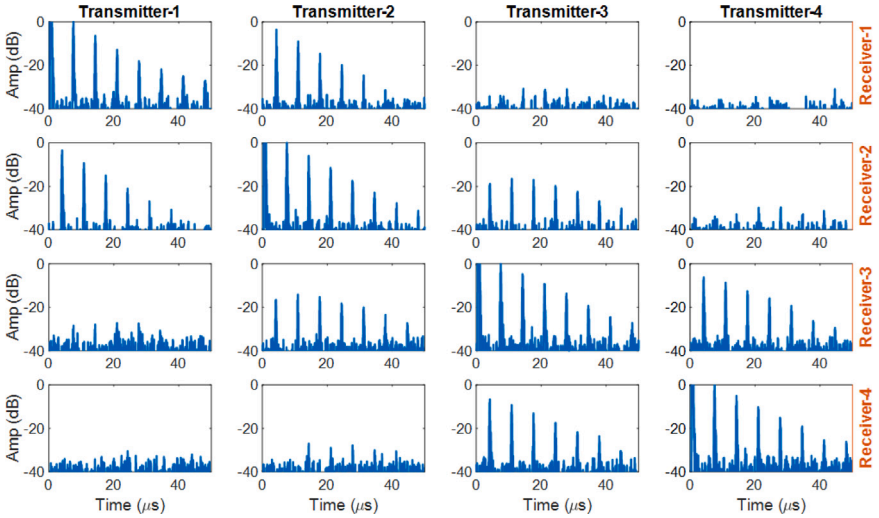


Fig. 15. Full matrix of A-scan signals on 4 contact transducers from the 2-facing-2 multi-channel experimental setup (shown in Fig. 13) using $L = 4002$ TOP-CS sequences with an $M = 4$ family (giving 200 μs orthogonal window) – showing full matrix of filtered signals to highlight the ability to locate propagation paths across channels from a single excitation event.

duration no longer limited by the arrival of useful information, aperiodic application of (odd-)periodic sequences can be used to allow the low-voltage system to outperform traditional systems without any increase to the signal dead-zone or introducing filter artefacts.

When combining the alternative hardware approach presented here ($\simeq \pm 2$ V peak transmission amplitude and acquisition range) with TOP coded excitations, contact transducer measurements matching the SNR (45 dB for the first echo) from commercial grade high-voltage pulsers (200 V unipolar pulse excitation with 15 dB of receiver gain) can be achieved whilst maintaining a 454 Hz PRF (sequence length of $L = 10008$) and reducing peak transmission power by 40 dB. Similarly, the front-wall SNR in an immersion setup using high-voltage equipment (45 dB again) can be matched whilst achieving a $\geq$1 kHz PRF (sequence length of $L = 2004$).

This paper has further shown how quasi-orthogonal sequence families can be produced via the Circularly-Shifted production method. With TOP-CS codes, complete crosstalk suppression in a set measurement window can be achieved for an arbitrary number of channels in a MIMO ultrasonic application. This was demonstrated experimentally using a 2-facing-2 grid of contact transducers to show, for the first time, how a full matrix capture of all the possible signals can be achieved in a single excitation event without cross-channel ultrasonic interference. The use of TOP-CS codes allows for the proposed low-power architecture to near match the performance of conventional systems in terms of signal quality and PRF in MIMO applications.

The low-power system results presented in this work were recorded with a laboratory grade AFG and oscilloscope. Given the simplicity of the proposed novel architecture – a pulser requiring only simple low-power high-speed bipolar symbols and the complete removal of active components on the receiver – a multi-channel low-power acquisition system can be conceived which opens the way for equally capable but much more cost effective and compact ultrasonic inspection hardware.

Finally, the experimental work presented here focused on ultrasound NDE applications with single-element pulse-echo transducer configurations. The low-power approach combined with TOP-CS sequence families can extend to phased array measurements, thus allowing the technique to be suitable for additional ultrasound NDE and medical applications. Similarly, TOP-CS codes can have further uses as they can be applied in pitch-catch or dual-element pulse-echo configurations without the need to change acquisition hardware.

CRediT authorship contribution statement

Connor Challinor: Conceptualization, Formal analysis, Investigation, Methodology, Writing – original draft. **Neil Pearson:** Supervision, Writing – review & editing. **Frederic Cegla:** Conceptualization, Formal analysis, Funding acquisition, Methodology, Supervision, Writing – review & editing.

Declaration of competing interest

The authors declare the following financial interests/personal relationships which may be considered as potential competing interests: Connor Challinor reports financial support was provided by NDT Global. Connor Challinor has patent #GB2304842.4 pending to Imperial College Innovations Limited. Frederic Cegla has patent #GB2304842.4 pending to Imperial College Innovations Limited.

Data availability

Data will be made available on request.

Acknowledgements

The authors would like to acknowledge funding from NDT Global, Germany and the EPSRC, UK via the FIND CDT (EP/S023275/1). Furthermore, we would like to thank Antonio De-Sanctis for his technical support in the laboratory. Finally, we would like to thank former and current supporters at NDT Global, Jochen Giese and Michael Haas, for their assistance in project supervision and useful discussions.

References

[1] E. García, J.A. Paredes, F.J. Álvarez, M.C. Pérez, J.J. García, Spreading sequences in active sensing: A review, Signal Process. 106 (2015) 88–105, http://dx.doi.org/10.1016/j.sigpro.2014.07.002.
[2] C. Cooke, The early history of pulse compression radar-the history of pulse compression at sperry gyroscope company, IEEE Trans. Aerosp. Electron. Syst. 24 (6) (1988) 825–833, http://dx.doi.org/10.1109/7.18654.
[3] A. Mudukutore, V. Chandrasekar, R. Keeler, Pulse compression for weather radars, IEEE Trans. Geosci. Remote Sens. 36 (1) (1998) 125–142, http://dx.doi.org/10.1109/36.655323.
[4] M. Parlak, M. Matsuo, J.F. Buckwalter, Analog signal processing for pulse compression radar in 90-nm CMOS, IEEE Trans. Microw. Theory Tech. 60 (12) (2012) 3810–3822, http://dx.doi.org/10.1109/TMTT.2012.2222433.
[5] S. Hedayatrasa, G. Poelman, J. Segers, W. Van Paepegem, M. Kersemans, Novel discrete frequency-phase modulated excitation waveform for enhanced depth resolvability of thermal wave radar, Mech. Syst. Signal Process. 132 (2019) 512–522, http://dx.doi.org/10.1016/j.ymssp.2019.07.011.
[6] J. Tang, W. Zhu, X. Qiu, A. Song, Y. Xiang, F.-Z. Xuan, Non-contact phase coded excitation of ultrasonic lamb wave for blind hole inspection, Ultrasonics 119 (2022) 106606, http://dx.doi.org/10.1016/j.ultras.2021.106606.
[7] M.K. Rizwan, S. Laureti, H. Mooshofer, M. Goldammer, M. Ricci, Ultrasonic imaging of thick carbon fiber reinforced polymers through pulse-compression-based phased array, Appl. Sci. 11 (4) (2021) http://dx.doi.org/10.3390/app11041508.
[8] F. Nicolet, D. Bujoreanu, E. Carcreff, H. Liebgott, D. Friboulet, B. Nicolas, Simultaneous coded plane-wave imaging using an advanced ultrasound forward model, Appl. Sci. 12 (24) (2022) http://dx.doi.org/10.3390/app122412809.
[9] J. Hua, L. Zeng, J. Lin, L. Huang, Excitation series design and pulse compression synthesis for high-resolution lamb wave inspection, Struct. Health Monit. 18 (5–6) (2019) 1464–1478, http://dx.doi.org/10.1177/1475921718801996.
[10] D. Hutchins, P. Burrascano, L. Davis, S. Laureti, M. Ricci, Coded waveforms for optimised air-coupled ultrasonic nondestructive evaluation, Ultrasonics 54 (7) (2014) 1745–1759, http://dx.doi.org/10.1016/j.ultras.2014.03.007.
[11] Z. Fan, X. Niu, B. Miao, H. Meng, Hybrid coded excitation of the torsional guided wave mode T(0,1) for oil and gas pipeline inspection, Appl. Sci. 12 (2) (2022) http://dx.doi.org/10.3390/app12020777.
[12] M. Ricci, L. Senni, P. Burrascano, R. Borgna, S. Neri, M. Calderini, Pulse-compression ultrasonic technique for the inspection of forged steel with high attenuation, Insight: Non-Destruct. Test. Condition Monitor. 54 (2012) 91–95, http://dx.doi.org/10.1784/insi.2012.54.2.91.
[13] F. Cegla, B. Herdovics, Coded excitation, motion and signal-to-noise ratio, in: 2018 IEEE International Symposium on Circuits and Systems, ISCAS, 2018, pp. 1–4, http://dx.doi.org/10.1109/ISCAS.2018.8351579.
[14] J. Isla, F. Cegla, Coded excitation for pulse-echo systems, IEEE Trans. Ultrason. Ferroelectr. Freq. Control 64 (4) (2017) 736–748, http://dx.doi.org/10.1109/TUFFC.2017.2661383.
[15] D. Lines, E. Mohseni, Y. Javadi, C. Mineo, R. Vithanage, Z. Qiu, C. MacLeod, G. Pierce, A. Gachagan, Using coded excitation to maintain signal to noise for FMC+TFM on attenuating materials, in: 2019 IEEE International Ultrasonics Symposium, IUS, 2019, pp. 635–638, http://dx.doi.org/10.1109/ULTSYM.2019.8925564.
[16] A. Nowicki, I. Trots, P. Lewin, W. Secomski, R. Tymkiewicz, Influence of the ultrasound transducer bandwidth on selection of the complementary golay bit code length, Ultrasonics 47 (1) (2007) 64–73, http://dx.doi.org/10.1016/j.ultras.2007.07.003.
[17] J.A. Isla, F.B. Cegla, Simultaneous transmission and reception on all elements of an array: Binary code excitation, Proc. R. Soc. A: Math. Phys. Eng. Sci. 475 (2019) http://dx.doi.org/10.1098/rspa.2018.0831.
[18] A. Bernieri, L. Ferrigno, M. Laracca, A. Rasile, M. Ricci, Ultrasonic NDT on aluminum bars: An experimental performance comparison of excitation and processing techniques, Measurement 128 (2018) 393–402, http://dx.doi.org/10.1016/j.measurement.2017.10.040.
[19] R. Challis, V. Ivchenko, R. Al-Lashi, Ultrasonic attenuation measurements at very high SNR: Correlation, information theory and performance, J. Phys. Conf. Ser. 457 (2013) http://dx.doi.org/10.1088/1742-6596/457/1/012004.
[20] M. Ricci, L. Senni, P. Burrascano, Exploiting pseudorandom sequences to enhance noise immunity for air-coupled ultrasonic nondestructive testing, IEEE Trans. Instrum. Meas. 61 (11) (2012) 2905–2915, http://dx.doi.org/10.1109/TIM.2012.2200409.
[21] R. Mulaveesala, S. Venkata Ghali, Coded excitation for infrared non-destructive testing of carbon fiber reinforced plastics, Rev. Sci. Instrum. 82 (5) (2011) 054902, http://dx.doi.org/10.1063/1.3594551.
[22] J. Hua, J.E. Michaels, X. Chen, J. Lin, Simultaneous excitation system for efficient guided wave structural health monitoring, Mech. Syst. Signal Process. 95 (2017) 506–523, http://dx.doi.org/10.1016/j.ymssp.2017.03.036.
[23] L. De Marchi, A. Marzani, J. Moll, P. Kudela, M. Radzieński, W. Ostachowicz, A pulse coding and decoding strategy to perform lamb wave inspections using simultaneously multiple actuators, Mech. Syst. Signal Process. 91 (2017) 111–121, http://dx.doi.org/10.1016/j.ymssp.2016.12.014.
[24] H. Zhang, S. Wu, D. Ta, K. Xu, W. Wang, Coded excitation of ultrasonic guided waves in long bone fracture assessment, Ultrasonics 54 (5) (2014) 1203–1209, http://dx.doi.org/10.1016/j.ultras.2013.10.020.
[25] E.P. Vienneau, B.C. Byram, A coded excitation framework for high SNR transcranial ultrasound imaging, IEEE Trans. Med. Imaging (2023) 1, http://dx.doi.org/10.1109/TMI.2023.3269022.
[26] L. Tong, Q. He, A. Ortega, A. Ramalli, P. Tortoli, J. Luo, J. D'hooge, Coded excitation for crosstalk suppression in multi-line transmit beamforming: Simulation study and experimental validation, Appl. Sci. 9 (3) (2019) http://dx.doi.org/10.3390/app9030486.
[27] T. Misaridis, J. Jensen, Use of modulated excitation signals in medical ultrasound. Part I: basic concepts and expected benefits, IEEE Trans. Ultrason. Ferroelectr. Freq. Control 52 (2) (2005) 177–191, http://dx.doi.org/10.1109/TUFFC.2005.1406545.
[28] T. Misaridis, J. Jensen, Use of modulated excitation signals in medical ultrasound. Part II: design and performance for medical imaging applications, IEEE Trans. Ultrason. Ferroelectr. Freq. Control 52 (2) (2005) 192–207, http://dx.doi.org/10.1109/TUFFC.2005.1406546.
[29] T. Misaridis, J. Jensen, Use of modulated excitation signals in medical ultrasound. Part III: high frame rate imaging, IEEE Trans. Ultrason. Ferroelectr. Freq. Control 52 (2) (2005) 208–219, http://dx.doi.org/10.1109/TUFFC.2005.1406547.

[30] X. Wang, J. Yang, J. Ji, Y. Zhang, S. Zhou, Research on golay-coded excitation in real-time imaging of high frequency ultrasound biomicroscopy, Sci. Rep. 11 (2021) http://dx.doi.org/10.1038/s41598-020-80406-x.
[31] R.P. Zangabad, J.G. Bosch, F. Mastik, R.H.S.H. Beurskens, V.A. Henneken, J.W. Weekamp, A.F.W. van der Steen, G. van Soest, Real-time coded excitation imaging using a CMUT-Based side looking array for intravascular ultrasound, IEEE Trans. Ultrason. Ferroelectr. Freq. Control 68 (6) (2021) 2048–2058, http://dx.doi.org/10.1109/TUFFC.2021.3054971.
[32] J.A. Flynn, L. Pflugrath, P. Kaczkowski, R.E. Daigle, Coded excitation reconstruction by impulse response estimation and retrospective acquisition, in: 2015 IEEE International Ultrasonics Symposium, IUS, 2015, pp. 1–6, http://dx.doi.org/10.1109/ULTSYM.2015.0125.
[33] T. Kaddoura, R.J. Zemp, Hadamard aperiodic interval codes for parallel-transmission 2D and 3D synthetic aperture ultrasound imaging, Appl. Sci. 12 (10) (2022) http://dx.doi.org/10.3390/app12104917.
[34] I. Trots, A. Nowicki, Y. Tasinkevych, M. Lewandowski, Golay coded sequences in synthetic aperture imaging systems, Arch. Acoust. 36 (4) (2011) 913–926, http://dx.doi.org/10.2478/v10168-011-0061-5.
[35] M.-H. Bae, W.-Y. Lee, M.-K. Jeong, S.-J. Kwon, Orthogonal golay code based ultrasonic imaging without reducing frame rate, in: 2002 IEEE Ultrasonics Symposium Proceedings, Vol. 2, 2002, pp. 1705–1708 vol.2, http://dx.doi.org/10.1109/ULTSYM.2002.1192625.
[36] R. Chiao, L. Thomas, Synthetic transmit aperture imaging using orthogonal golay coded excitation, in: 2000 IEEE Ultrasonics Symposium Proceedings, Vol. 2, 2000, pp. 1677–1680 vol.2, http://dx.doi.org/10.1109/ULTSYM.2000.921644.
[37] I. Trots, Mutually orthogonal golay complementary sequences in synthetic aperture imaging systems, Arch. Acoust. 40 (2) (2015) 283–289, http://dx.doi.org/10.1515/aoa-2015-0031.
[38] B.-H. Kim, T.-K. Song, Multiple transmit focusing using modified orthogonal golay codes for small scale systems, in: IEEE Symposium on Ultrasonics, 2003, Vol. 2, 2003, pp. 1574–1577, http://dx.doi.org/10.1109/ULTSYM.2003.1293208.
[39] M. Yang, C. Chakrabarti, Design of orthogonal coded excitation for synthetic aperture imaging in ultrasound systems, in: 2012 IEEE International Symposium on Circuits and Systems, ISCAS, 2012, pp. 113–116, http://dx.doi.org/10.1109/ISCAS.2012.6271430.
[40] R. Chiao, X. Hao, Coded excitation for diagnostic ultrasound: a system developer's perspective, IEEE Trans. Ultrason. Ferroelectr. Freq. Control 52 (2) (2005) 160–170, http://dx.doi.org/10.1109/TUFFC.2005.1406543.
[41] E. Vienneau, B. Byram, Compound barker-coded excitation for increased signal-to-noise ratio and penetration depth in transcranial ultrasound imaging, in: 2020 IEEE International Ultrasonics Symposium, IUS, 2020, pp. 1–4, http://dx.doi.org/10.1109/IUS46767.2020.9251650.
[42] B. Zejak, I. Simic, A. Zejak, Matched and mismatched pulse compression in medical ultrasound imaging, in: EUROCON'2001. International Conference on Trends in Communications. Technical Program, Proceedings (Cat. No.01EX439), vol. 2, 2001, pp. 333–336 vol.2, http://dx.doi.org/10.1109/EURCON.2001.938128.
[43] G. Turin, An introduction to matched filters, IRE Trans. Inf. Theory 6 (3) (1960) 311–329, http://dx.doi.org/10.1109/TIT.1960.1057571.
[44] P. Burrascano, S. Callegari, A. Montisci, M. Ricci, M. Versaci, M. Tucci, Ultrasonic nondestructive evaluation systems: industrial application issues, Ultrasonic Nondestructive Evaluation Systems: Industrial Application Issues, Springer Science+Business Media, New York, New York, 2015.
[45] J. Choi, S. Youn, J.Y. Hwang, S. Ha, C. Kim, M. Je, Energy-efficient high-voltage pulsers for ultrasound transducers, IEEE Trans. Circuits Syst. II 68 (1) (2021) 19–23, http://dx.doi.org/10.1109/TCSII.2020.3040548.
[46] D. Sarwate, M. Pursley, Crosscorrelation properties of pseudorandom and related sequences, Proc. IEEE 68 Issue 5 (1980) 593–619.
[47] J. Jedwab, A survey of the merit factor problem for binary sequences, in: Proceedings of 3rd International Conference on Sequences and their Applications, SETA'04, 2004.
[48] M. Golay, Sieves for low autocorrelation binary sequences, IEEE Trans. Inform. Theory 23 (1) (1977) 43–51, http://dx.doi.org/10.1109/TIT.1977.1055653.
[49] M. Golay, Complementary series, IRE Trans. Inf. Theory 7 (2) (1961) 82–87, http://dx.doi.org/10.1109/TIT.1961.1057620.
[50] M.G. Parker, K.G. Paterson, C. Tellambura, Golay complementary sequences, in: Wiley Encyclopedia of Telecommunications, John Wiley & Sons, Ltd, 2003, http://dx.doi.org/10.1002/0471219282.eot367, arXiv:https://onlinelibrary.wiley.com/doi/pdf/10.1002/0471219282.eot367.
[51] PeakN.D.T. Ltd, MicroPulse LT2 - product page, 2023, https://www.peakndt.com/products/micropulse-lt2/.
[52] N. Xiang, Using M-sequences for determining the impulse responses of LTI-systems, Signal Process. 28 (2) (1992) 139–152, http://dx.doi.org/10.1016/0165-1684(92)90031-Q.
[53] S.W. Golomb, Shift Register Sequences, 3rd Revised, WORLD SCIENTIFIC, 2017, http://dx.doi.org/10.1142/9361, arXiv:https://www.worldscientific.com/doi/pdf/10.1142/9361.
[54] H. Luke, H. Schotten, Odd-perfect, almost binary correlation sequences, IEEE Trans. Aerosp. Electron. Syst. 31 (1) (1995) 495–498, http://dx.doi.org/10.1109/7.366335.
[55] P. Ke, S. Zhang, F. Lin, Constructions of binary array set with zero-correlation zone, Inform. Sci. 197 (2012) 197–206, http://dx.doi.org/10.1016/j.ins.2012.02.010.
[56] B. Fassi, A. Djebbari, A. Taleb-Ahmed, Ternary zero correlation zone sequence sets for asynchronous DS-CDMA, Commun. Netw. 06 (2014) 209–217, http://dx.doi.org/10.4236/cn.2014.64023.
[57] H.D. Lüke, Sets of ternary sequences with odd-periodic zero correlation zones, Frequenz 58 (9–10) (2004) 214–216, http://dx.doi.org/10.1515/FREQ.2004.58.9-10.214.